Gate-bias assisted charge injection in organic field-effect transistors

Brondijk, J. J.; Torricelli, F.; Smits, E. C. P.; Blom, P. W. M.; de Leeuw, D. M.

IMPORTANT NOTE: You are advised to consult the publisher's version (publisher's PDF) if you wish to cite from it. Please check the document version below.

Document Version
Publisher's PDF, also known as Version of record

[Link to publication in University of Groningen/UMCG research database](#)
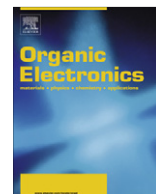
Gate-bias assisted charge injection in organic field-effect transistors

J.J. Brondijk [a,*], F. Torricelli [b], E.C.P. Smits [c], P.W.M. Blom [a,c], D.M. de Leeuw [a,d]

[a] Molecular Electronics, Zernike Institute for Advanced Materials, University of Groningen Nijenborgh 4, 9747 AG Groningen, The Netherlands
[b] Department of Electrical Engineering, Eindhoven University of Technology, 5600 MB Eindhoven, The Netherlands
[c] TNO Holst Centre, P.O. Box 8550, 5605 KN Eindhoven, The Netherlands
[d] Philips Research Laboratories, High Tech Campus 4, 5656 AE Eindhoven, The Netherlands

ABSTRACT

The charge injection barriers in organic field-effect transistors (OFETs) seem to be far less critical as compared to organic light-emitting diodes (OLEDs). Counter intuitively; we show that the origin is image-force lowering of the barrier due to the gate bias at the source contact; although the corresponding gate field is perpendicular to the channel current. In coplanar OFETs; injection barriers up to 1 eV can be surmounted by increasing the gate bias; enabling extraction of bulk transport parameters in this regime. For staggered transistors; however; the injection is gate-assisted only until the gate bias is screened by the accumulation channel opposite to the source contact. The gate-assisted injection is supported by two-dimensional numerical charge transport simulations that reproduce the gate-bias dependence of the contact resistance and the typical S-shaped output curves as observed for OFETs with high injection barriers.

© 2012 Elsevier B.V. All rights reserved.

1. Introduction

The current in an organic light-emitting diode (OLED) strongly depends on the charge injection barrier [1–5]. The injection barrier is taken as the energy difference between the workfunction of the electrode and the highest occupied molecular orbital (HOMO) or lowest unoccupied molecular orbital (LUMO) energy of the organic semiconductor. When the barrier is less than about 0.25 eV; the current is bulk limited [5]. In that case; the maximum current that is electrostatically allowed is the space-charge limited current. When the injection barrier is larger than 0.25 eV the current is injection limited; the bulk current cannot be supplied by the contact. The diode current typically decreases by an order of magnitude for each 0.25 eV increase in barrier height [6]. Hence to maximize the current and efficiency in OLEDs matching between the workfunction of the electrode and the HOMO or LUMO energy of the semiconductor is crucial.

In organic field-effect transistors (OFETs) the nature of the contact seems less important. There are numerous examples showing that the charge transport in transistors is rather tolerant for injection barriers. Pentacene has been investigated using transistors with source and drain electrodes with widely different work functions: Au;Cu;Ni. Surprisingly; the saturated output currents differed by less than an order of magnitude [7]. Extreme examples are ambipolar transistors; using a single electrode material to inject both electrons and holes; where considerable current is measured even with injection barriers larger than 0.5 eV [8–10].

In OFETs the contact resistance depends on the barrier height at the metal-semiconductor interface; but it also strongly dependents on the biases; the transistor architecture and geometry. In particular; the contact resistance reduces with increasing gate-bias [7,11–13] and with increasing temperature [14,15]. Severely contact limited transistors show an S-shaped output curve (current vs. drain bias; I_D vs. V_D); with a nonlinear diode-like behavior at low drain bias [12,14,16,17]. Coplanar transistors usually have a higher contact resistance with respect to their

* Corresponding author. Tel.: +31 50 363 5211; fax: +31 50 363 8751.
   *E-mail address:* j.j.brondijk@rug.nl (J.J. Brondijk).

staggered counterpart [16]. In staggered transistors the contact resistance was attributed to the current-crowding effect and to a gate-dependent bulk resistance [18–20]. In a coplanar structure the contact resistance has been explained as the combined effect of a Schottky contact and a field-dependent mobility [21,22]. Although these physical effects enable a good modeling of the transistor characteristics;they are not able to explain why an OFET is more insensitive to the barrier height than an OLED [11–13].

Here we show that the observed difference between charge injection in an OLED and in an OFET is implicitly due to the gate bias. A quantitative analysis of the charge transport requires a model to describe the charge injection into a disordered organic semiconductor. Various models have been reported [21,23–26]; but a final consensus has not yet been reached. As a first order approximation we use thermionic emission [27]. We show that by including image-force lowering the tolerance of charge transport in an OFET to the injection barrier can be quantitatively explained. Transfer and output curves are reproduced and the consequences for parameter extraction are discussed. Coplanar and staggered OFETs with the same geometrical and physical parameters are analyzed and compared.

2. Methods

We take a unipolar p-type field-effect transistor with an undoped semiconductor; i.e. we assume a background doping density not higher than 10^{16} cm^{-3} [28]; as shown in the inset of Fig. 1a. At zero gate bias the OFET can basically be considered as a lateral OLED. The source-drain bias of typically a few volts is distributed over the channel with a typical length of a few micrometer. As a result the source-drain field in an OFET is typically 2–3 orders of magnitude lower than the electric field in an OLED. Due to the much lower electric field; the associated image-force lowering can be neglected; the injection barrier is then equal to the difference between the electrode work-function and the HOMO energy of the semiconductor. In p-type OFETs the source is grounded; whereas the drain is operated at a small negative bias. Consequently; holes are injected from the source contact. The energy barrier at the drain contact can be disregarded since for hole extraction this barrier does not play a role; as also demonstrated by scanning Kelvin probe potentiometry measurements [29].

To investigate the role of the gate bias on the charge injection; we calculated the carrier density; electric potential; and the resulting current in a p-type transistor. To quantify the injection by the source contact; we implemented classical thermionic emission by defining the boundary condition for the hole current as: $J_p = (AT^2/N_V)(p - p_0)$ where A is the effective Richardson constant; T the absolute temperature; N_V the effective density of states in the semiconductor and p the hole density. The equilibrium hole density depends on the effective barrier for holes; φ_B; and it is given by $p_0 = N_V exp(-\varphi_B/k_B T)$; where k_B is the Boltzmann constant. For thermionic emission without barrier lowering; the effective barrier; φ_B; is equal to the initial barrier; φ_{B0}: the energy difference
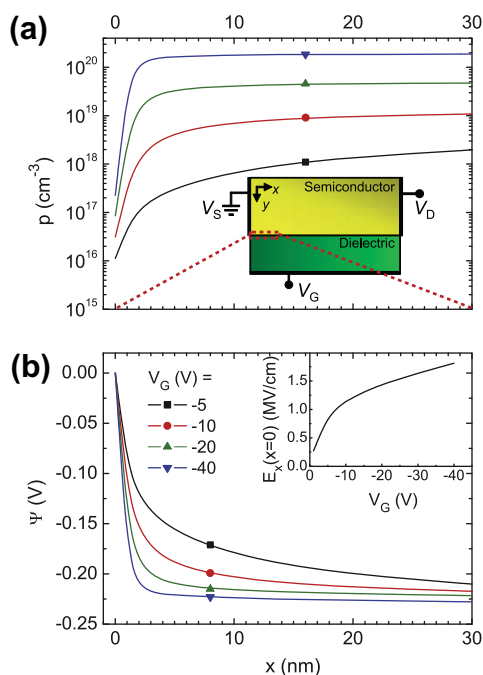
Fig. 1. (a) Hole density and (b) local electrostatic potential; ψ; in the channel of an injection limited p-type bottom-contact bottom-gate (coplanar) transistor with an initial injection barrier φ_{B0} = 0.5 eV. Density and potential are plotted versus distance from the source contact; x; at the semiconductor-dielectric interface; as a function of gate bias. Inset in (a): schematic representation of a bottom-contact bottom-gate field-effect transistor. Inset in (b): the electric field in the x-direction at the source contact; at the dielectric interface; versus gate bias. The drain bias was −2 V; the channel length and width were 20 μm and 1 mm; the hole mobility was 0.01 cm^2/Vs; the effective Richardson constant was 100 A K^{-2} cm^{-2};and the gate capacitance 17 nF/cm^{-2}.

between the electrode work function and the HOMO energy. If image-force lowering is taken into account; then the effective barrier decreases. The barrier lowering is a function of the electric field at the source contact; E; and reads [27]: $\Delta\varphi = e\sqrt{eE/(4\pi\varepsilon_S)}$ where $\varepsilon_S = \varepsilon_0\varepsilon_{SC}$ is the semiconductor permittivity and e is the elementary charge.

In order to model the hole injection into the semiconductor a two-dimensional (2D) device simulator is required. The current in the transistor can be calculated by defining a 2D mesh and iteratively solving at each point Poisson's equation; the continuity equations and the drift-diffusion equations. For this purpose we used the 2D device simulator CURRY [30–32]; where thermionic emission in combination with image-force lowering is implemented. We note that at low temperatures or at very high electric fields additional injection mechanisms such as thermally-assisted tunneling or Fowler-Nordheim tunneling might be operative [29]. For simplicity these mechanisms are disregarded. Furthermore; in order to disentangle gate-bias assisted injection from effects due to a field- and density dependent mobility we use a constant mobility in this study. In this sense our approach differs from [21]; where the interdependence of contact properties and field- and density-dependent mobility in OFETs has been studied but unfortunately barrier lowering

was neglected. It is worth noting that; in general; both Schottky barrier lowering and the field- and density-dependent mobility can contribute to contact effects.

3. Results and discussion

In order to elucidate the role of V_G on the charge injection; we start our analysis considering a bottom-contact bottom-gate OFET; as schematically depicted in Fig 1. The local hole density and potential as a function of the distance from the source contact are plotted for different V_G; in Fig. 1; in equilibrium. When a gate bias is applied; holes with a concentration of $C_i V_G$; with C_i the gate capacitance per unit area; are accumulated in the channel; which becomes conductive. However; due to the injection barrier the hole concentration strongly drops close to the source contact and a depletion region is formed; as shown in Fig. 1a. As a result the source-drain bias mainly drops over this depletion region at the source contact. For increasing gate bias; the depletion region narrows; as shown in Fig. 1b. This can be explained as follows: The depletion width depends on the charge carrier concentration in the semiconductor; that is modulated by the gate bias according to $C_i V_G$. A higher V_G thus gives a larger concentration; thereby reducing the depletion width of the reverse-biased Schottky diode. As shown in the inset of Fig. 1b the reduction of the width of the space-charge region is accompanied by an increase of the lateral electric field at the contact; E_x. Hence; the effective barrier lowers by the image force effect and the injected current is higher. A smaller part of the drain-source bias; V_D; drops over the contact. In principle; by applying a large enough gate bias; the field will be eventually high enough to supply the current demanded by the bulk. We note that the injection limited curves will never completely reach the bulk limited curve; because a small part of V_D will always drop over the contact. In summary; the electric field at the source contact is responsible for the barrier lowering and the field is implicitly modulated by the gate bias.
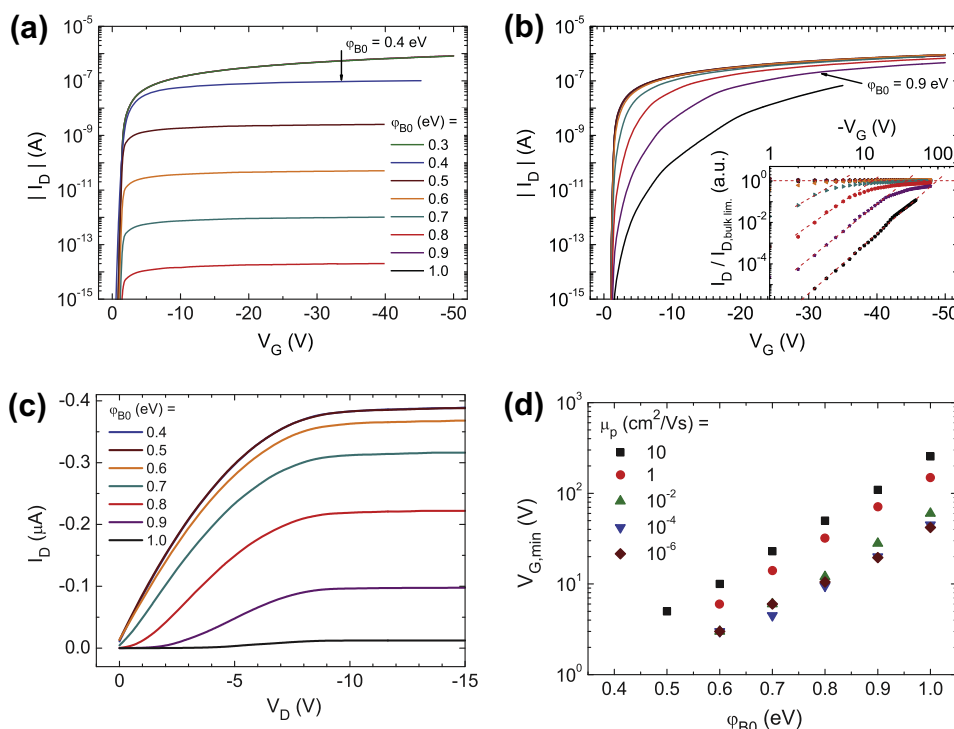
Transfer curves calculated without image-force lowering as a function of initial barrier height are presented in Fig. 2a. For the calculations we took a typical value for the channel length of 20 μm. For much larger channels the bulk channel resistance is dominant and at much smaller lengths short channel effects might dominate [33–36]. The analysis of short channel effects is beyond the scope of this work. As expected; for barriers up to 0.3 eV the calculated transfer curves are identical; the current is bulk limited. At higher barriers the current becomes injection limited. The current decreases exponentially with increasing barrier height; about 60 mV/decade. This value differs from the experimental value derived from OLEDs; 250 mV/decade; presumably due to the incorrect assumption of thermionic emission as the dominating injection mechanism. A model based on thermally assisted hopping from the electrode into the localized states of the organic semiconductor; which are broadened due to disorder; is probably more realistic [26]; but mathematically hard to implement in the 2D device solver. The thermionic emission implemented here leads to a similar basic understanding of the gate-bias assisted injection process in OFETs.

Without image force lowering the transfer curves saturate with increasing gate bias; as shown in Fig. 2a. As a comparison; transfer curves calculated including image-force lowering are presented in Fig. 2b. At low gate bias; the calculated current strongly depends on the initial barrier height; similar to the OLED case. However; as the gate bias increases; the calculated currents almost converge due to the gate-bias assisted image-force lowering. Hence at low gate bias the current is injection limited; while at high bias the current becomes bulk limited. This indicates that in the case of bottom-contact bottom-gate transistors the mobility values extracted in the linear regime at high gate bias approach the bulk value. Furthermore; the contact resistance for a given barrier height can be calculated from Fig. 2b. For instance at large barriers we can ignore the bulk channel resistance. The contact resistance is then approximately equal to the drain bias divided by the drain current. Fig. 2b therefore indicates that the contact resistance drops with gate bias; in good agreement with literature data [7,11–13]. Thus; without barrier lowering the effective barrier is equal to the initial barrier independent of the gate bias. Hence; the transfer curves saturate and do not converge. When barrier lowering is taken into account the effective barrier decreases with increasing gate bias. Hence the difference in calculated currents gets smaller; and at very high gate bias the calculated currents converge.

The role of the drain-source bias is elucidated in Fig. 2c; where the output curves are presented as a function of initial barrier height. The output currents are calculated including image-force lowering. It appears that for barriers up to 0.5 eV the calculated curves are identical. At low drain bias the current increases linearly with drain bias; the extracted mobility is constant and equal to the nominal bulk mobility. With increasing barrier height; the current has a superlinear; diode-like dependence on V_D at low drain bias and the current is almost perfectly flat at large drain bias. Consequently; the output curves at high barrier height show an S-shape; as experimentally observed in severely contact limited transistors [12,14,16,17]. The origin is that for a given gate bias the barrier lowering increases with source-drain bias; since the total field at the source contact is enhanced. The S-shape has previously been attributed to an electric field dependent mobility [21,22]. Here we show that a large injection barrier described by thermionic emission and image-force lowering alone is sufficient. We note that calculations without barrier lowering only result in a reduced current; but not in a different shape.

In the limit of infinite gate bias; all injection barriers in a coplanar transistor can be surmounted; as shown in Fig. 2b. Practical questions are what is the minimum gate bias needed to overcome the barrier; $V_{G,min}$; and how this bias depends on the bulk mobility. To estimate the minimum gate bias we replot the transfer curves on a double logarithmic scale as shown in the inset of Fig. 2b. The current is normalized to the bulk current as calculated without injection barrier. Hence for barriers below about 0.3 eV a straight line at unity is obtained. For higher barriers the current at low bias is injection limited and an

Fig. 2. Simulated transfer curves of a *p*-type bottom-contact bottom-gate (coplanar) transistor as a function of initial injection barrier; at a drain bias of −2 V. The calculations were performed (a) without and (b) with image-force barrier lowering at the source contact. Inset in (b): the current at each gate bias normalized to the bulk-limited current; obtained for zero barrier; at the corresponding bias. The dotted lines are a guide to the eye. (c) Calculated output curves; including image-force lowering; as a function of the initial injection barrier at the source; φ_{B0}; at $V_G = -10$ V. (d) The calculated gate bias required to overcome the injection barrier; $V_{G,\min}$; versus the initial injection barrier; φ_{B0}; as a function of the hole mobility; μ_p. The drain bias was −2 V. The parameters such as bulk mobility; capacitance; channel length and width are identical to those of Fig. 1.

apparent power law dependence is obtained. The intersection of the extrapolated power law with the bulk normalized current is taken as $V_{G,\min}$. The values derived are presented in Fig. 2d as a function of initial barrier height. At low barrier height the minimum gate bias is negligible. The minimum gate bias is calculated to increase almost exponentially with barrier height; which is expected from the exponential dependence of the thermionic emission on injection barrier height.

As an example; Fig. 2d shows that for low mobility semiconductors; μ_p; lower than about 10^{-2} cm^2/Vs; barriers of for instance 0.8 eV can be overcome at a gate bias of about 10 V. This indicates that the mobility values extracted at higher gate biases approach the bulk value. Mobility values extracted at low bias can be orders of magnitude lower. We note that in an OLED the mobility cannot reliably be extracted for high injection barriers without having a detailed knowledge on the injection mechanism. Fig. 2d shows that for high-mobility semiconductors a higher minimum gate bias is needed to overcome a similar barrier. In fact; an increased mobility results in a higher channel current; which has to be supplied by the contact. The analysis suggests that although much research effort is directed towards high-mobility materials; the best performance can only be achieved with a good balance between charge injection and current transport.

In order to investigate the role of the transistor geometry in gate-bias assisted injection we extend the analysis to

the case of staggered top-contact bottom-gate OFETs. The transistor structure is shown in the inset of Fig. 3d. The channel width and length and the physical parameters of the semiconductor are identical to those used for the coplanar OFET discussed above. The width of the source and drain electrodes is 2 μm. Transfer curves calculated without image-force lowering as a function of the initial barrier height are presented in Fig. 3a. For barriers up to 0.4 eV the calculated transfer curves are identical and the current is bulk limited. At higher barriers the current becomes injection limited. It is worth noting that the bulk-limited transfer curves obtained for the staggered OFET (Fig. 3a) are identical to those calculated for the coplanar OFET in Fig. 2a, the curves have the same magnitude and shape. In the case of the staggered structure; the barrier height after which the current becomes injection limited is slightly higher than the one obtained for the coplanar transistor. This is because for staggered OFETs; with the gate and electrodes on opposite sides of the semiconductor; the effective injection region is a few orders of magnitude larger than for coplanar OFETs; where the injection region is only the side of the contact next to the nanometer-scale transport channel.

Calculated transfer curves including image-force lowering are presented in Fig. 3b. For the staggered geometry the current is injection limited for barriers higher than 0.6 eV. Comparing the results plotted in Fig. 3a and b; the calculated current including barrier lowering becomes injection
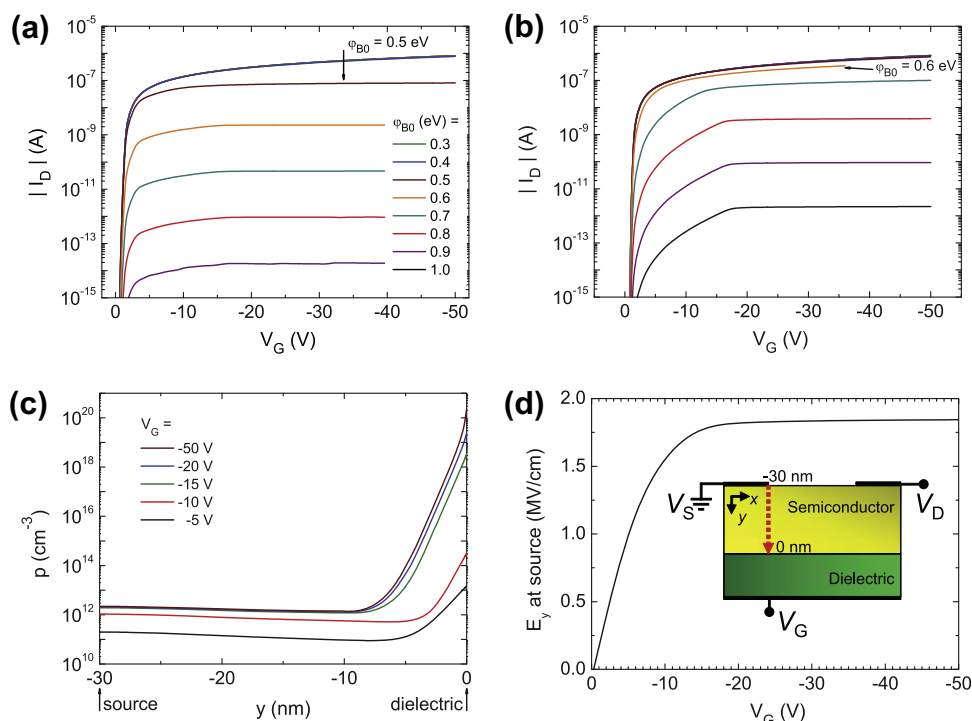
Fig. 3. Simulated transfer curves of a p-type top-contact bottom-gate (staggered) transistor as a function of initial injection barrier; at a drain bias of −2 V. The calculations were performed (a) without and (b) with image-force barrier lowering at the source contact. (c) Hole density along the vertical y-direction at the source contact; along the red dashed line in the inset in (d); with an initial barrier ϕ_{B0} = 0.8 eV. (d) The electric field in the y-direction at the source contact; versus the gate bias. Inset: schematical representation of a top-contact bottom-gate field-effect transistor. The width of the source and drain electrodes is 2 μm and all the other parameters not specified; such as the bulk mobility; gate capacitance; channel length and width; are identical to those of Fig. 1. (For interpretation of the references to colour in this figure legend, the reader is referred to the web version of this article.)

limited at higher barriers. This confirms that the gate bias also has a beneficial effect on the charge injection in staggered transistors. At small gate bias the current strongly increases with V_G; whereas after a certain value of the gate bias ($|V_G|$ > 15 V in Fig. 3b) it becomes independent of V_G. This agrees with the results reported in [20]. However; the gate-assisted injection is much weaker than in the coplanar transistor and a nearly Ohmic injection cannot be achieved at very high values of V_G. In order to investigate this point; we plot in Fig. 3c the hole concentration along the vertical direction at the source as a function of gate bias. For small values of V_G ($|V_G|$ < 15 V) the hole concentration at the metal-semiconductor interface is modulated by the gate bias; which explains the strong current increase with V_G in Fig. 3b. However; for high gate bias; the accumulated charge at the semiconductor-dielectric interface screens the gate bias. This screening results in a constant hole concentration at the source contact; at the opposite side of the semiconductor; in agreement with previously reported electrostatic simulations [37].

The electric field at the injecting source contact as a function of the gate bias is presented in Fig. 3d. When $|V_G|$ is larger than about 20 V; the gate bias is fully screened by the accumulated channel and the electric field at the contact remains constant. Therefore; we can conclude that in staggered OFETs the injection is gate-bias assisted until the channel opposite to the source contact is fully accumu-

lated. How effective the screening is depends on the semiconductor thickness. By varying the semiconductor thickness; we verified that the gate-assistance is less pronounced for thicker layers. The provided analysis physically explains why the "contact effects" are different in coplanar and staggered transistors. The underlying physics is basically the same; but the role of the injecting contact and channel depends strongly on the transistor geometry.

4. Summary

In summary; in an OLED the injection barrier should be below 0.3 eV to achieve bulk limited transport. In contrast; an OFET is much more tolerant for injection barriers. The origin is image-force lowering of the barrier due to the high electric field at the source contact. In a coplanar OFET under accumulation the electric field at the source contact progressively increases with increasing gate bias. At low gate bias the source contact limits the injection. However; by increasing the gate bias injection barriers up to 1 eV can be surmounted and extracted parameter values resemble those of the bulk semiconductor. 2D numerical simulations reproduce the typical S-shape output curves of OFETs with high injection barriers without any further assumptions. In a staggered OFET the injection is gate-bias enhanced until the accumulated channel; opposite to the source contact; screens the gate bias.

Acknowledgements

References

[1] B.K. Crone, I.H. Campbell, P.S. Davids, D.L. Smith, C.J. Neef, J.P. Ferraris, J. Appl. Phys. 86 (1999) 5767.
[2] G.G. Malliaras, J.C. Scott, J. Appl. Phys. 85 (1999) 7426.
[3] T. van Woudenbergh, P.W.M. Blom, M.C.J.M. Vissenberg, J.N. Huiberts, Appl. Phys. Lett. 79 (2001) 1697.
[4] T. van Woudenbergh, P.W.M. Blom, J.N. Huiberts, Appl. Phys. Lett. 82 (2003) 985.
[5] P.W.M. Blom, M.J.M. de Jong, J.J.M. Vleggaar, Appl. Phys. Lett. 68 (1996) 3308.
[6] K. Asadi, T.G. de Boer, P.W.M. Blom, D.M. de Leeuw, Adv. Funct. Mater. 19 (2009) 3173–3178.
[7] D.J. Gundlach, L. Zhou, J.A. Nichols, T.N. Jackson, P.V. Necliudov, M.S. Shur, J. Appl. Phys. 100 (2006) 024509.
[8] E.C.P. Smits, T.D. Anthopoulos, S. Setayesh, E. van Veenendaal, R. Coehoorn, P.W.M. Blom, B. de Boer, D.M. de Leeuw, Phys. Rev. B 73 (2006) 205316.
[9] T.D. Anthopoulos, C. Tanase, S. Setayesh, E.J. Meijer, J.C. Hummelen, P.W.M. Blom, D.M. de Leeuw, Adv. Mater. 16 (2004) 2174–2179.
[10] L. Bürgi, M. Turbiez, R. Pfeiffer, F. Bienewald, H.-J. Kirner, C. Winnewisser, Adv. Mater. 20 (2008) 2217–2224.
[11] K.P. Puntambekar, P.V. Pesavento, C.D. Frisbie, Appl. Phys. Lett. 83 (2003) 5539.
[12] M. Kitamura, S. Aomori, J.H. Na, Y. Arakawa, Appl. Phys. Lett. 93 (2008) 033313.
[13] K. Nakayama, T. Uemura, M. Uno, J. Takeya, Appl. Phys. Lett. 95 (2009) 113308.
[14] B.H. Hamadani, D. Natelson, J. Appl. Phys. 97 (2005) 064508.
[15] B.H. Hamadani, D. Natelson, Appl. Phys. Lett. 84 (2004) 443.
[16] R.A. Street, A. Salleo, Appl. Phys. Lett. 81 (2002) 2887.
[17] N. Kawasaki, Y. Ohta, Y. Kubozono, A. Fujiwara, Appl. Phys. Lett. 91 (2007) 123518.
[18] T.J. Richards, H. Sirringhaus, J. Appl. Phys. 102 (2007) 094510.
[19] N. Tessler, Y. Roichman, Appl. Phys. Lett. 79 (2001) 2987.
[20] V. Vinciguerra, M. La Rosa, D. Nicolosi, G. Sicurella, L. Occhipinti, Org. Electron. 10 (2009) 1074–1081.
[21] S. Scheinert, G. Paasch, J. Appl. Phys. 105 (2009) 014509.
[22] A. Bolognesi, A. Di Carlo, P. Lugli, Appl. Phys. Lett. 81 (2002) 4646.
[23] M. Koehler, I. Biaggio, M. da Luz, Phys. Rev. B 78 (2008) 153312.
[24] J.K.J. van Duren, V.D. Mihailetchi, P.W.M. Blom, T. van Woudenbergh, J.C. Hummelen, M.T. Rispens, R.A.J. Janssen, M.M. Wienk, J. Appl. Phys. 94 (2003) 4477.
[25] J. Scott, G.G. Malliaras, Chem. Phys. Lett. 299 (1999) 115–119.
[26] V.I. Arkhipov, E.V. Emelianova, Y.H. Tak, H. Bässler, J. Appl. Phys. 84 (1998) 848.
[27] S.M. Sze;K.K. Ng;Physics of Semiconductor Devices;3rd Edition;Wiley-Interscience;2006.
[28] J.J. Brondijk, M. Spijkman, F. van Seijen, P.W.M. Blom, D.M. de Leeuw, Phys. Rev. B 85 (2012) 165310.
[29] L. Bürgi, T.J. Richards, R.H. Friend, H. Sirringhaus, J. Appl. Phys. 94 (2003) 6129.
[30] S.J. Polak, C. den Heijer, W.H.A. Schilders, P. Markowich, Int. J. Numer. Methods Eng. 24 (1987) 763–838.
[31] A. Heringa, M.M.A. Driessen, J.M.F. Peters, W.H.A. Schilders, COMPEL: Int, J. Comput. Math. Electr. Electron. Eng. 10 (1991) 621–630.
[32] J.J. Brondijk, M. Spijkman, F. Torricelli, P.W.M. Blom, D.M. de Leeuw, Appl. Phys. Lett. 100 (2012) 023308.
[33] J. Haddock, X. Zhang, S. Zheng, Q. Zhang, S. Marder, B. Kippelen, Org. Electron. 7 (2006) 45–54.
[34] F.D. Fleischli, K. Sidler, M. Schaer, V. Savu, J. Brugger, L. Zuppiroli, Org. Electron. 12 (2011) 336–340.
[35] S. Locci, M. Morana, E. Orgiu, A. Bonfiglio, P. Lugli, IEEE Trans. Electron Devices 55 (2008) 2561–2567.
[36] M.L. Chabinyc, J.-P. Lu, R.A. Street, Y. Wu, P. Liu, B.S. Ong, J. Appl. Phys. 96 (2004) 2063.
[37] T. Li, J.W. Balk, P.P. Ruden, I.H. Campbell, D.L. Smith, J. Appl. Phys. 91 (2002) 4312.